Article

Hydrogen Production from Methane in Atmospheric Non-Equilibrium Plasma

Hiroshi Yamada[1,a,*]**, Tatsuya Yamamoto**[1]**, Tomohiko Tagawa**[2,b]**, Katsutoshi Nagaoka**[1,c]

1 Chemical Systems Engineering, Nagoya university, Furo-cho, Chikusa-ku, Nagoya-shi, 464-8603, Japan
2 National institute of technology, Toyota college, Eisei-cho 2-1, Toyota-shi, 471-8525, Japan
E-mail: [a,*]yamada.hiroshi@material.nagoya-u.ac.jp (Corresponding author), [b]tagawa@toyota-ct.ac.jp, [c]nagaoka.katsutoshi@material.nagoya-u.ac.jp

Abstract. The instability of supplied power is a serious problem for chemical plants in developing countries. An easy start-up/shut-down system is important in this situation. The present report describes a hydrocarbon decomposition system using nonequilibrium plasma for hydrogen production. A microwave oven was used as a preliminary microwave reactor, which contained a quartz glass tube that passed through the top panel to the bottom panel of the microwave oven. Argon and methane flow were directed into the reactor, where the argon gas became plasma in the tube. A carbon stick was set in the tube as the excitation material of argon to plasma. Initially, the reaction was conducted under a methane partial pressure of 200 hPa. The main products were hydrogen and acetylene, with a small amount of ethylene also produced. Conversion and yields decreased with increasing methane partial pressure. Hydrogen production rate initially increased with methane partial pressure, but then decreased. The optimum methane partial pressure was determined. Gas flow rate had no effect on conversion or yield. The reactant and products reached an equilibrium state as soon as the reactant was introduced to the plasma. Pure hydrogen, 95%, was obtained by adjusting the experimental conditions.

Keywords: Hydrogen production, atmospheric non-equilibrium plasma, microwave, argon.

This article is based on the presentation at the International Conference on Engineering and Industrial Technology (ICEIT 2020) in Chonburi, Thailand, 11th-13th September 2020.

1. Introduction

Hydrogen is produced by steam reforming of hydrocarbons [1-3]. However, this process also produces carbon dioxide, which is one of the causes of global warming. Some reports describe the use of carbon dioxide instead of steam [4-6], but carbon dioxide formed even in this dry reforming system. Capturing carbon dioxide and storing it in an underground is one solution for reducing carbon dioxide, which is currently under investigation [7-9].

Hydrocarbons contain hydrogen and carbon atoms. The direct removal of hydrogen from hydrocarbons would allow the production of hydrogen while fixing carbon.

The use of hydrocarbons as a resource for reactions has a major problem of carbon deposition on the catalyst surface [10-12]. However, this problem could also be viewed as the fixation of carbon on the catalyst surface. Upham [13] proposed the use of molten metals catalyst for hydrogen production. In this process, the carbon was skimmed off and pure hydrogen was produced.

Power supply instability can be a serious problem for chemical plants in developing country [14]. An easy start-up/shut-down system is important in this situation. In general, catalytic processes require complex procedures for start-up and shut-down. Frequent black outs are detrimental to chemical plant systems, and deactivation/ acceleration at every start-up and shut-down [15-17] cannot be ignored.

This report describes a hydrocarbon decomposition system using nonequilibrium plasma for hydrogen production. Nonequilibrium plasma is low-temperature plasma, nearly room temperature. Only electrons have high energy. These high-energy electrons activate hydrocarbons and break the carbon-hydrogen bond. Hydrogen atoms become hydrogen gas and carbon atoms become solid carbon. This is a noncatalytic system that has simple and rapid start-up and shut-down operations.

Some reports on low pressure nonequilibrium plasma have been published [18, 19], but few involve atmospheric pressure nonequilibrium plasma. The possibility of hydrogen production using atmospheric nonequilibrium plasma was examined in this study.

2. Experimental

Microwave activated electrons of argon gas resulted in the gas becoming nonequilibrium plasma. A microwave oven, Haier Jm-17E 2.45GhZ 700W, was used as a simple microwave reactor. Although the actual power of the oven was unknown, the actual power to the tube reactor was constant during the experiments. A quartz glass tube, 30 mm in diameter, passed through the top panel to the bottom panel of the microwave oven. The length of the tube in the oven cabinet was 20 cm. Figure 1 shows the plasma reactor schematic. Argon and methane gas flowed into the reactor where the argon gas became plasma in the tube. Reaction was conducted at atmospheric pressure.

The total flow rate of argon and methane was fixed at 300 cm³/min. Flow rate of each gas was maintained to control the partial pressure of methane. The reaction temperature was unknown, because a thermocouple could not be placed in the microwave oven. A carbon stick, 6 cm in length and 0.5 mm in diameter, was set in the tube and was used as the excitation material to promote argon to a plasma. Outlet flow rate was measured using a soap film meter and the product concentration was measured by TCD-GC (GL-Science Inc. GC-323). The outlet molar flow rate was calculated from these values.
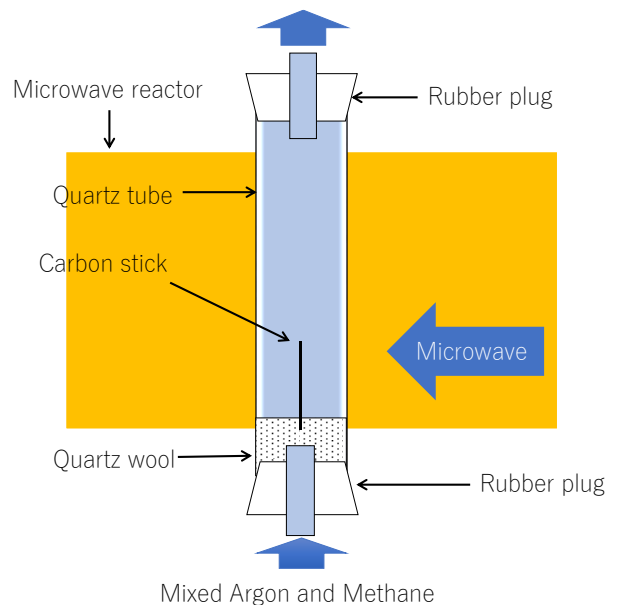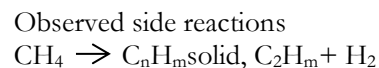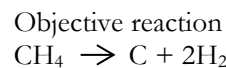

Fig. 1. Reactor schematic diagram.

Reactions in the reactor were as follows.

Objective reaction
$$CH_4 \rightarrow C + 2H_2$$

Observed side reactions
$$CH_4 \rightarrow C_nH_m\text{solid}, C_2H_m + H_2$$

Conversion and yields were calculated using the following equation:

Methane conversion, X_{CH4}

X_{CH4} = (inlet methane molar flow rate - outlet methane molar flow rate) / inlet methane molar flow rate

Hydrogen yield, Y_{H2}

Y_{H2} = 2 x outlet hydrogen molar flow rate / 4 x (inlet methane molar flow rate - outlet methane molar flow rate)

Ethane, ethylene, and acetylene yield, Y_{C2H6}, Y_{C2H4}, Y_{C2H2}

Y_{C2H6}, Y_{C2H4}, Y_{C2H2} = 2 x molar outlet flow rate of each material / (inlet methane molar flow rate - outlet methane molar flow rate)
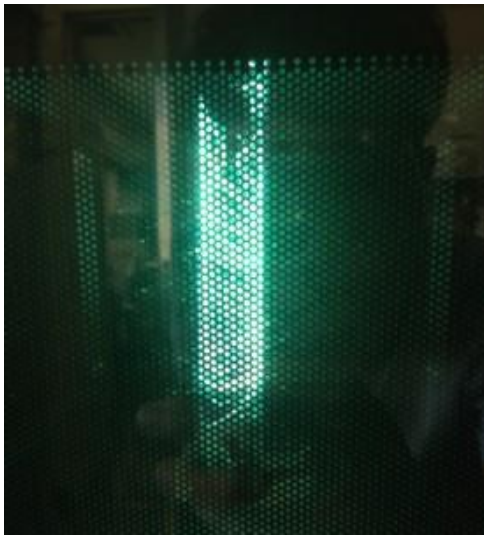
Material balance

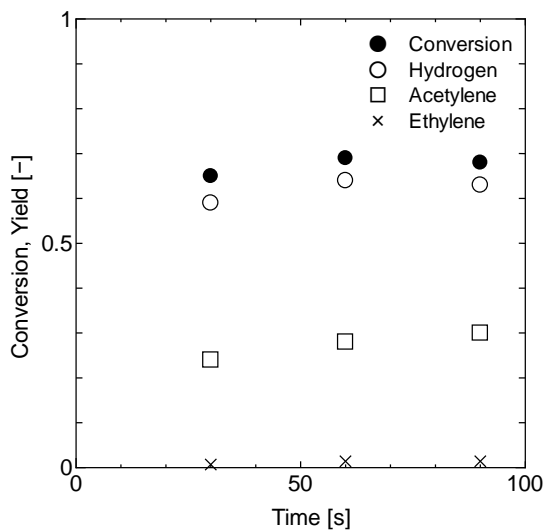Fig. 2. Nonequilibrium argon plasma in the tube.

Fig. 3. Reaction profiles at the methane partial pressure of 200 hPa.

Carbon balance = carbon atom number of each material in outlet molar flow / inlet methane molar flow rate

Hydrogen balance = Hydrogen atom number of each material in outlet molar flow / 4 x inlet methane molar flow rate

3. Results and Discussions

3.1. Standard Condition

Initially, only methane flowed into the reactor. No reaction occurred and no light emission was observed in the reactor. Then, only argon flowed into the reactor. Bright green light emission was observed in the reactor. Microwave radiation generated nonequilibrium argon plasma. Figure 2 shows the nonequilibrium argon plasma in the reactor tube. Without the carbon stick, plasma was not generated. The carbon stick was required to excite argon to plasma. Microwave ovens normally heat all of the

materials in the oven because the microwaves are dispersed and do not focus on one point. The electric field in a microwave oven is not strong enough to excite argon to plasma. The carbon stick diffracted microwaves to increase field intensity around the stick. The carbon stick absorbed microwaves and emitted electrons, which excited the argon gas.

At first, the reaction was conducted at a methane partial pressure of 200 hPa. Figure 3 shows product yields and methane conversion. Conversion and product yields were stable before 90 seconds. The argon plasma became smaller and vanished after 90 seconds. The carbon deposited on the tube wall absorbed microwaves [20]. The carbon stick could not absorb enough microwaves. Figure 4 shows the deposited carbon. Carbon also deposited on the carbon stick tip. Absorbed electrons were emitted from the edge of the stick. Deposited carbon covered the edge. Electron emission was inhibited. These two carbon depositions caused the disappearance of the plasma. The main products were hydrogen and acetylene, along with a small amount of ethylene. The same products were formed when low-pressure nonequilibrium plasma was used [21]. Figure 5 shows the material balance. The hydrogen balance was 1 while the carbon balance was 0.6. This result indicates that the deposited black solid was carbon, not hydrocarbon.

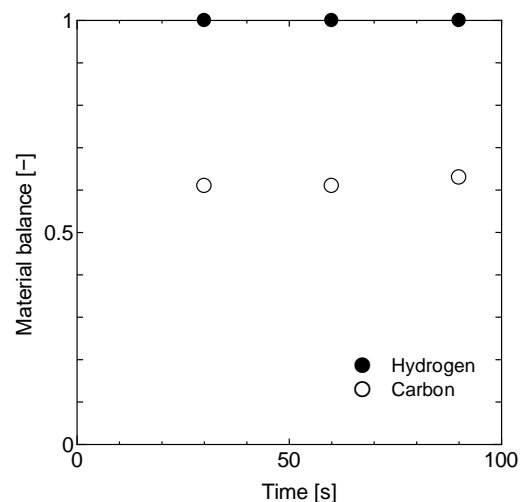Fig. 4. Carbon deposited on the tube inner wall.

Fig. 5. Material balance for hydrogen and carbon at the methane partial pressure of 200 hPa.

Table 1 shows the effect of methane partial pressure on the argon plasma. Bright green plasma was observed until 150 hPa. The color turned to white and the plasma field decreased. A white color in the emission spectroscopy is indicative of methane intermediates. Eventually, no emission was observed and the carbon stick appeared to be red-hot. Methane inhibited the excitation of argon to plasma.

Table 1. Effect of methane partial pressure on the plasma.

Methane partial pressure (hPa)	98	150	200	254	302
Conversion	0.89	0.78	0.62	0.53	0.33
Plasma color	Green	Green	Green+White	Green+White	White~Redheat

Figure 6 shows the effect of methane partial pressure on conversion and product yields, which decreased as methane partial pressure increased. An increase in methane partial pressure increased inlet methane molar flow rate and decreased methane residence time. In general, methane residence time affects conversion in many tubular reactors. However, flow rate did not affect conversion in this system. This point was discussed in the section 3.3. Decreasing argon plasma volume caused a decrease in conversion and yields. Methane partial pressure had no effect on the product distribution.
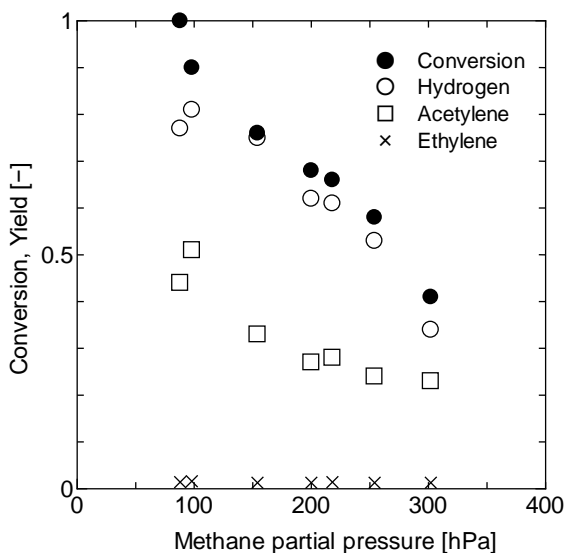

Fig. 6. Effect of methane partial pressure on the reaction.

Figure 7 shows the effect of methane partial pressure on hydrogen production rate. Hydrogen production rate initially increased with methane partial pressure, but eventually decreased. The maximum value was 80 cm^3/min. Increasing methane flow rate and decreasing

hydrogen yields resulted in this maximum value. An optimum methane partial pressure also was determined.
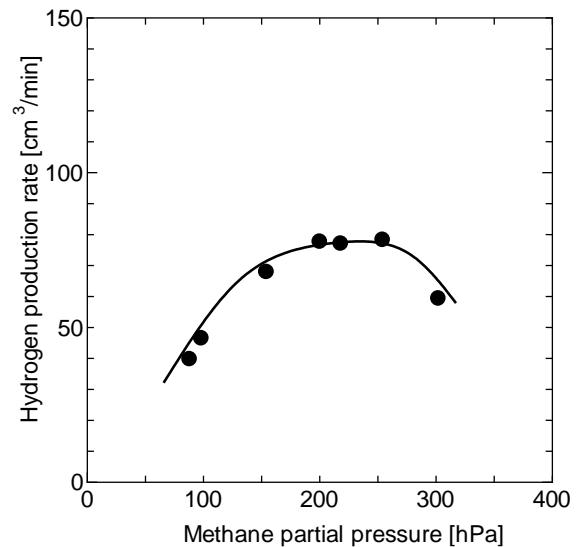

Fig. 7. Effect of methane partial pressure on hydrogen production rate.

3.2. Reaction Mechanism

Methane was converted to CH*, C*, H*, and others in the plasma. These active species collided and formed products. Some intermediates collided with the tube wall and formed solid carbon. Table 2 [22] shows the binding energy for each bond. A carbon-carbon single bond possesses lower energy than a carbon-hydrogen bond. A carbon-carbon triple bond has greater energy than a double or single bond. Thus, acetylene is more difficult to produce than ethane or ethylene. However, acetylene was the major product among these three hydrocarbons. Carbon bonds were activated and split again in the plasma, but the activation energy was not high enough to split the carbon-carbon triple bond. Thus, only acetylene remained in the plasma. Carbon atoms were converted to acetylene and solid carbon. Remaining hydrogen atoms became hydrogen molecules after leaving the plasma.

Table 2. Binding energy of carbon and hydrogen.

	Binding energy, kJ/mol
C —C	344
C —H	415
H —H	436
C =C	615
C ≡C	812

3.3. Effect of Gas Flow Rate and Direction

Gas flow rate was varied to control residence time. Figure 8 shows the effect of gas flow rate on conversion

and yields. The methane partial pressure was 220 hPa. Gas flow rate had no effect on these values. Reaction rate in the plasma field was very high. Reactant and products reached an equilibrium as soon as reactant was introduced to the plasma. Hydrogen production rate increased linearly.

Deposited carbon inhibited continuous plasma production. When the gas flow direction was reversed, the carbon deposition location was expected to move, but the result was the same as in the standard experiment.

Argon and methane mixed gas was supplied to the carbon stick during the standard experiment. Methane around the carbon stick resulted in carbon deposition near the location of the carbon stick. The methane supplying tube was extended to the middle of the reactor tube, which resulted in the argon plasma being produced at the bottom of the tube and then transferred to the methane inlet. This represents a simple model of a commercial microwave reactor. Continuous plasma production was expected and a larger plasma area was observed. But, a high concentration of methane around the methane inlet extinguished the plasma, indicating that a higher energized plasma was required. The location of the carbon deposition leaved exciting material. Stable reaction time was enhanced 1.5-fold, but conversion was decreased to 0.35. As mentioned earlier, this reactor cannot focus the microwaves to one point. Carbon deposition absorbed microwaves even far from the carbon stick. The electric field around the exciting material became weaker, indicating that separating the plasma production point and methane reaction point was effective for promoting continuous reaction. The commercial microwave reactor allowed focus of the microwaves on the one point, resulting in continuous plasma generation.
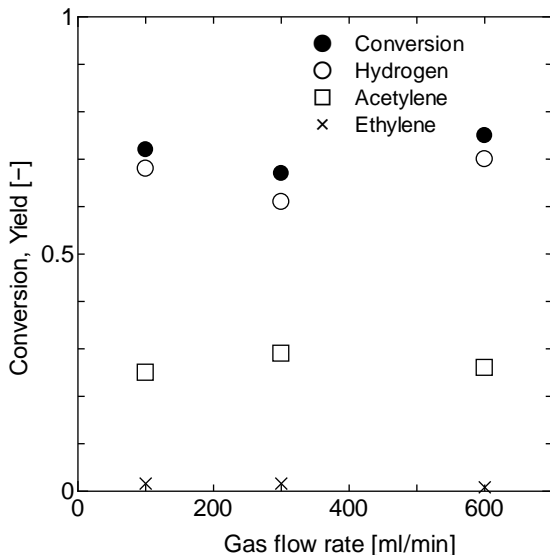

Fig. 8. Effect of gas flow rate on conversion.

3.4. Effect of Tube Diameter

To decrease gas phase thickness between tube wall and carbon stick and the amount of methane around the carbon stick, a smaller diameter reactor tube was used. Tube diameter was decreased from 30 mm to 20 mm.

Figure 9 shows the effect of methane partial pressure on conversion and yields using the 20-mm diameter quartz tube. The flow rate was the same as in previous experiments, i.e., 300 cm^3/min. Plasma was observed at high methane partial pressure. The amount of methane in the reactor tube decreased when using the 20-mm tube, and the carbon stick could absorb larger amounts of energy. The carbon stick emitted enough electrons to produce plasma, even at high methane pressures. These results are presented in Table 3. The amount of solid deposition on the tube wall was also increased. The hydrogen and carbon balance was 0.82 and 0.30, respectively. Their value was small compared to those obtained when using the 30-mm tube. The number of collisions of carbon active species with the tube wall was increased by using the 20-mm tube. Solid deposition is therefore believed to have increased with the number of collisions. In this narrow tube, the hydrogen balance was less than 1, indicating that either hydrocarbon was deposited instead of carbon or the deposited carbon adsorbed the hydrogen.

Table 3. Effect of methane partial pressure on the plasma.

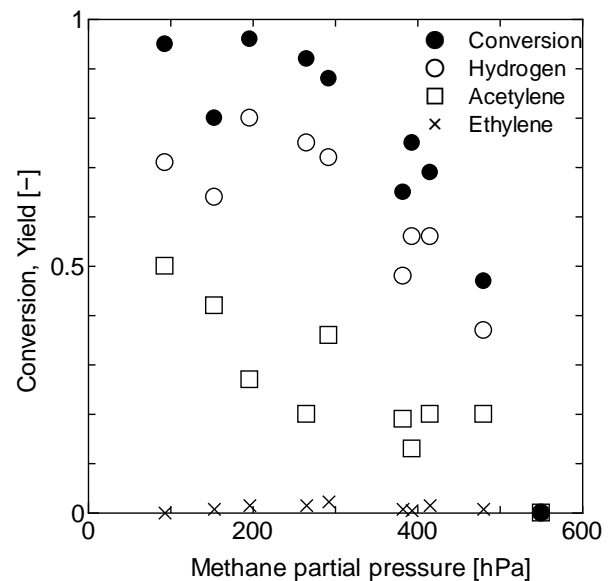| Methane partial pressure (hPa)	100	200	300	400	500
Conversion	1	0.95	0.85	0.68	0.42
Plasma color	Green		Green + White	White	

Fig. 9. Effect of methane partial pressure on the reaction when using a 20-mm tube.
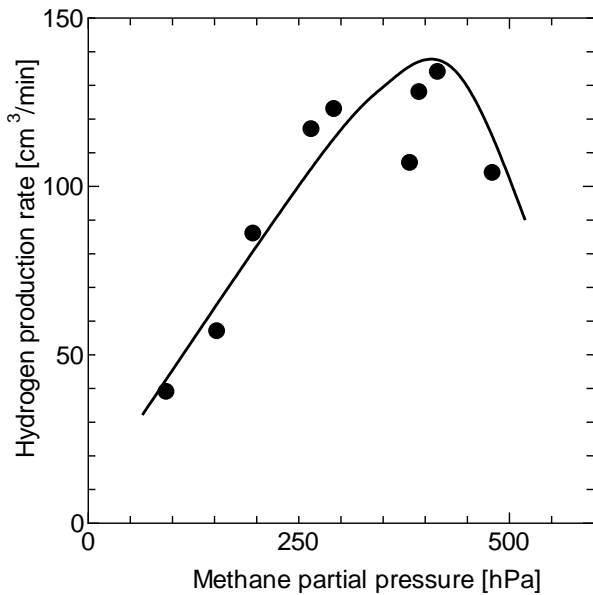
Fig. 10. Effect of methane partial pressure on hydrogen production rate when using a 20-mm tube.
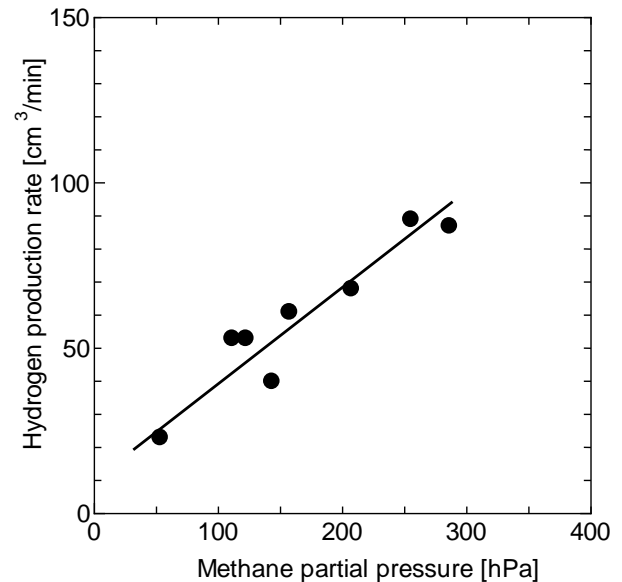

Fig. 12. Effect of methane partial pressure on hydrogen production rate when using an 8-mm tube.

Hydrogen production rate increased with methane partial pressure (Fig. 12). No decrease was observed in this range.

3.5. Position of Exciting Material

Use of a narrow tube promoted efficient plasma production. The thickness of the methane gas phase around the carbon stick was thin when a narrow tube was used and the carbon stick absorbed a large amount of energy. The effect of the distance from the tube wall to the carbon stick was varied. When the carbon stick was located near the tube wall, the distance from opposite side wall became longer. For these experiments, two carbon sticks were used, arranged in two patterns. One pattern had the carbon sticks located symmetrically along the wall sides. The other pattern had the two carbon sticks located in the center of the tube, slightly apart. Figure 13 shows the conversion profiles of the center pattern at a methane partial pressure of 230 hPa. Conversion and yields were nearly the same as those resulting when one carbon stick was used. The number of carbon sticks had no effect on the reaction. As with the effect of flow rate, one carbon stick is enough to allow the reaction to achieve equilibrium. Figure 14 shows the conversion profiles of wall pattern at a methane partial pressure of 230 hPa. Conversion was increased by moving the carbon sticks to the wall because the sticks absorbed greater energy and the plasma had stronger electric field intensity. With the carbon sticks against the tube wall, a lower acetylene yield occurred. A strong plasma field is powerful enough to split carbon-carbon triple bonds, so the carbon atoms stayed in an intermediate state until they hit the tube wall and were deposited as a solid. Little hydrocarbon was detected in the outlet flow, indicating that many of the carbon atoms were deposited as a solid. Pure hydrogen, 95%, was obtained under these conditions.
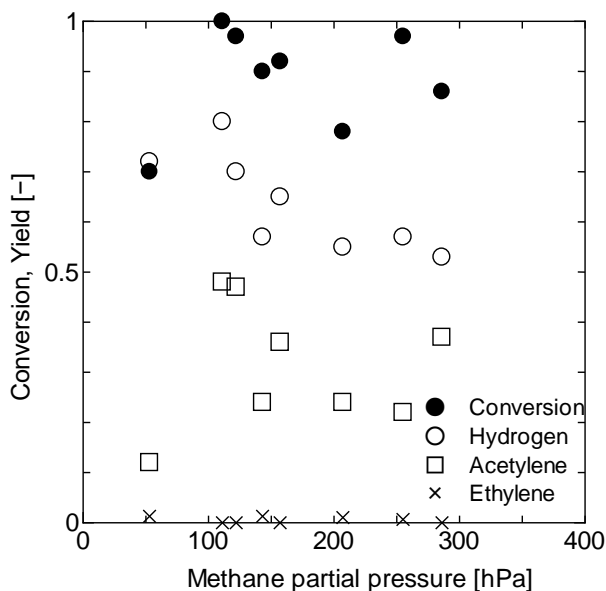

Fig. 11. Effect of methane partial pressure on the reaction when using an 8-mm tube.

Hydrogen production rate increased with methane partial pressure (Fig. 10), and then decreased. Maximum hydrogen production rate was 140 cm³/min, which was larger than that found using the 30-mm diameter tube.

Next, an even more narrow tube, 8 mm in diameter, was used. Figure 11 shows the effect of methane partial pressure on conversion and yield. Conversion was stable within the range, and exciting material absorbed more energy in this narrow tube. The hydrogen and carbon balances were 0.65 and 0.25, respectively. Mass balance decreased. The amount of solid deposition increased. The carbon deposits absorbed microwaves, resulting in the rapid extinguishing of the argon plasma at greater than 300 hPa.
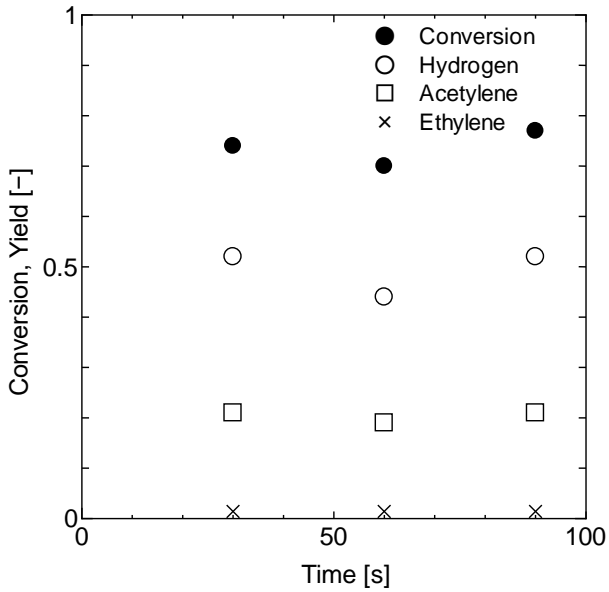
Fig. 13. Reaction profiles when using two carbon sticks located in the center of the reaction tube.
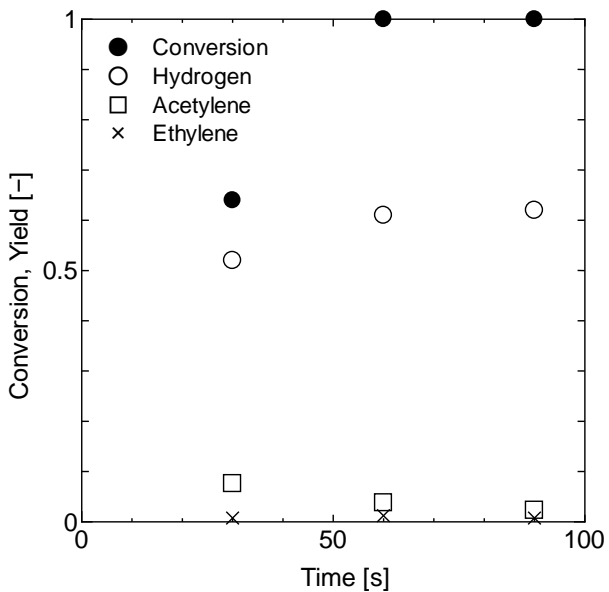

Fig. 14. Reaction profiles when using two carbon sticks located on the wall of the reaction tube.

3.6. Effect of Reactant

To investigate the use of various reactants, propane was used for the reaction. Figure 15 shows the reaction profile at a propane partial pressure of 100 hPa. Hydrogen and acetylene were the main products along with a small amount of methane. Molecules containing 3 carbon atoms, such as propylene, were not produced. The same products were detected when methane was used. Intermediates in the plasma were the same as when using methane. Carbon deposition on the tube wall was greater than when propane was used. Increasing the number of carbon atoms in the reactor increased the number of carbon atom collisions with the tube wall. The conversion value was

0.57, which was smaller than that for methane. Propane has more bonds than methane, and propane absorbed more energy than methane. Therefore, the plasma weakened. Acetylene yield from propane was greater than that from methane, partly due to the weaker plasma and to the amount of carbon atoms in the reactor. More carbon atoms result in more carbon-carbon collisions, which increase the likelihood of carbon-carbon triple bond formation.
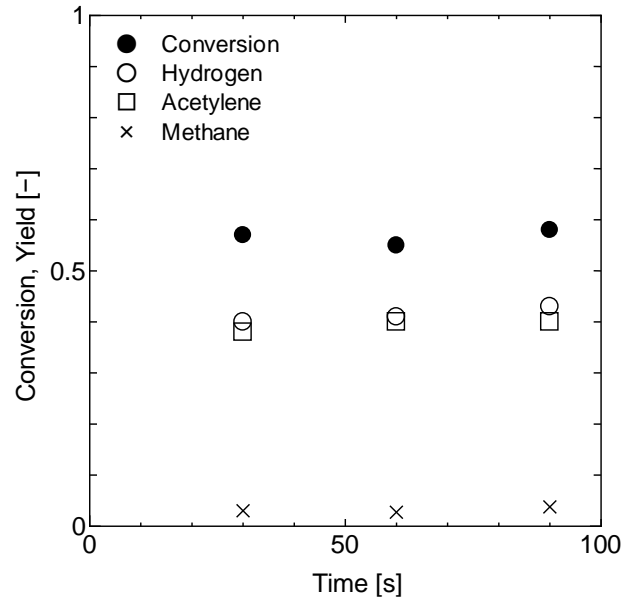

Fig. 15. Reaction profiles when propane was used as reactant.

4. Conclusions

Hydrogen production using nonequilibrium argon plasma was reported. Nonequilibrium plasma was made by microwave irradiation on argon gas. Pure hydrogen was obtained by adjusting the experimental conditions. Carbon also was fixed as a solid material. The amount of irradiation energy input to the argon gas was an important factor.

Because a preliminary microwave reactor was used, exciting material was required for focusing the microwaves on the argon gas. No exciting material should be needed when using a standard microwave reactor. In this case, the locations of nonequilibrium plasma generation and hydrocarbon reaction can be separated. Continuous hydrogen production is possible by spraying plasma onto hydrocarbon gas.

References

[1] S. R. de la Rama, S. Kawai, H. Yamada, and T. Tagawa, "Preliminary assesment of oxidation pretreated hastelloy as hydrocarbon steam reforming catalyst," *J catal.*, vol. 2014, 2014, Article ID 289071.

[2] D. Paschenko, "Numerical study of steam methane reforming over a pre-heated Ni-based catalyst with

detailed fluid dynamics," *Fuel*, vol. 236, pp. 686-694, 2019.

[3] B. V. R. Kuncharam, and A. G. Dixon, "Multi-scale two-dimensional packed bed reactor model for industrial steam methane reforming," *Fuel Process. Technol.*, vol. 200, 2020, Article ID 106314.

[4] S. R. de la Rama, H. Yamada, and T. Tagawa, "Effect of oxidation pretreatment temperature on kovar used as CO_2 reforming catalyst," *J. Fuel. Chem. Technol.*, vol. 42, pp. 573-581, 2014.

[5] N. N. Gavrilova, V. N. Sapunov, and V. V. Skudin, "Intensification of dry reforming of methane on membrane catalyst," *Chem. Eng. J.*, vol. 374, pp. 983-991, 2019.

[6] J. Dou, R. Zhang, X. Hao, Z. Bao, T. Wu, B. Wang, and F. YU, "Sandwiched $SiO_2@Ni@ZrO_2$ as a coke resistant nanocatalyst for dry reforming of methane," *Appl. Catal. B*, vol. 254, pp. 612-623, 2019.

[7] J. S. Lee and E. C. Choi, "CO_2 leakage environmental damage cost - A CCS project in South Korea," *Renew. Sust. Energ. Rev.*, vol. 93, pp. 753-758, 2018.

[8] A. Read, C. Gittins, J. Uilenreef, T. Jonker, F. Neele, S. Belfroid, E. Goetheerand, and T. Wildenborg, "Lessons from the ROAD project for future deployment of CCS," *Int. J. Greenh. Gas Control.*, vol. 91, 2019, Article ID 102834.

[9] Y. Tan, W. Nookuea, H. Li, E. Thorin, and J. Yan, "Property impacts on Carbon Capture and Storage (CCS) processes: A review," *Energy Convers. Manag.*, vol. 118, pp. 204-222, 2016.

[10] T. Tagawa, S. R. de la Rama, S. Kawai, and H. Yamada, "Partial oxidation catalyst derived from Ni containing alloy for biomass gasfication process," *Cem. Eng. Trans.*, vol. 32, pp. 583-588, 2013.

[11] V. Samano, M. S. Rana, and J. Ancheyta, "An easy approach based on textural properties to evaluate catalyst deactivation during heavy oil hydrotreating," *Catal. Commun.*, vol. 133, 2020, Article ID 105823.

[12] X. Li, P. Li. X. Pan, H. Ma, and X. bao, "Deactivation mechanism and regeneration of carbon nanocomposite catalyst for acetylene hydrochlorination," *Appl. Catal. B.*, vol. 210, pp. 116-120, 2017.

[13] D. C. Upham, V. Agarwal, A. Khechfe, Z. R. Snodgrass, M. J. Gordon, H. Metiu, and E. W. McFarland, "Catalytic molten metals for the direct conversion of methane to hydrogen and separable carbon," *Science*, vol. 358, pp. 917-921, 2017.

[14] JETRO Report, "Power situation and policies in Asia and Oceania," (in Japanease), 2015.

[15] H. Goshima, H. Yamada, T. Tagawa, and Y. Kawashima, "Deactivation of water gas shift catalyst due to DSS operation for PEFC applications," in *International symposium on EcoTopia Science 2007*, Nagoya, 2007.

[16] P. Guo, L. Chen, Q. Yang, M. Qiao, H. Li, H. Li, H. Xu, and K. Fan, "$Cu/ZnO/Al_2O_3$ water-gas shift catalysts for practical fuel cell applications: The performance in shut-down/start-up operation," *Int. J. Hydrog. Energy*, vol. 34, pp. 2361-2368, 2009.

[17] D. Li, K. Nishida, Y. Zhan, T. Shishido, Y. Oumi, T. Sano, and K. Takehira, "Superior catalytic behavior of trace Pt-doped Ni/Mg(Al)O in methane reforming under daily start-up and shut-down operation," *Appl. Catal. A.*, vol. 350, pp. 225-236, 2008.

[18] M. Capitelli, G. Colonna, G. D'Ammando, V. Laporta, and A. Laricchiuta, "The role of electron scattering with vibrationally excited nitrogen molecules on non-euilibrium plasma kinetics," *Phys. Plasmas*, vol. 20, 2013, Article ID 101609.

[19] T. Makabe and T. Yagisawa, "Low-pressure nonequilibrium plasma for a top-down nanoprocess," *Plasma Sources Sci. Thechnol.*, vol. 20, 2011, Article ID 024011.

[20] K. Oshima, "Mechanism and applications of microwave heating (Japanease)," *Shikizai*, vol. 44, pp. 27-35, 1971.

[21] K. Onoe, A. Fujie, T. Yamaguchi, and Y. Hatano, "Selective synthesis of acetylene from methane by microwave plasma reactions," *Fuel*, vol. 76, pp. 281-282, 1997.

[22] S. Tuchiya and A. Hirakawa, "Chemical binding energy," (in Japanese) in *Material Science, Reaction and Physical Property*. Tokyo, Japan: Foundation for the Promotion of the Open University of Japan, 1999, sec. 3-3, pp. 40-45.

Hiroshi Yamada, photograph and biography not available at the time of publication.

Tatsuya Yamamoto, photograph and biography not available at the time of publication.

Tomohiko Tagawa, photograph and biography not available at the time of publication.

Katsutoshi Nagaoka, photograph and biography not available at the time of publication.

Hiroshi Yamada, photograph and biography not available at the time of publication.